Received 10 September 2024
Revised 8 October 2024
Accepted 8 October 2024

Experimental study on the acoustic roughness spectrum of high-speed railway rails

Li Han and Xiangyang Wu
Institute of Energy Conservation, Environmental Protection, and Occupational Safety, China Academy of Railway Sciences Corporation Limited, Beijing, China
Qing Yu
Survey and Design Department, Beijing Rail Transit Construction and Management Co., Ltd, Beijing, China, and
Lanhua Liu and Chenge Wang
Institute of Energy Conservation, Environmental Protection, and Occupational Safety, China Academy of Railway Sciences Corporation Limited, Beijing, China

Abstract

Purpose – This study aims to investigate the acoustic roughness of rails on China's high-speed railways, with a focus on short-wavelength irregularities (less than 80 cm), which are known to significantly contribute to noise. The goal is to develop a specific acoustic roughness spectrum tailored for China's high-speed railway system, as no such spectrum currently exists.

Design/methodology/approach – A long-term tracking study was conducted on major railway lines in China, monitoring rail roughness throughout the initial operational period and the rails' service life. Data preprocessing techniques such as peak removal and curvature correction were applied for acoustic adjustments. A spatial-wavelength domain transformation was performed, providing the distribution patterns and statistical characteristics of acoustic roughness on China's high-speed rails. Based on these analyses, a model for constructing the acoustic roughness spectrum was developed.

Findings – The study found that the acoustic roughness of China's high-speed railway rails follows a χ^2 distribution with six degrees of freedom. For wavelengths greater than 8 cm, the acoustic roughness spectrum remains below the ISO specified limits. In the wavelength range of 3.2 cm to 6.3 cm, the roughness is comparable to or within the limits specified by ISO 3095:2005 and ISO 3095:2013. However, for wavelengths shorter than 2.5 cm, the roughness exceeds ISO limits.

Originality/value – This research fills the gap in the lack of a specific acoustic roughness spectrum for China's high-speed railways. By establishing a tailored spectrum based on long-term data analysis, the

This research project is supported by multiple funding sources, including the China State Railway Group Co., Ltd.'s Science and Technology Development Plan (Project Code: P2022Z003). The project aims to drive innovation and technological advancements in key areas of railway development. Besides, the research has received backing from the China Academy of Railway Sciences Co., Ltd. as part of their specialized research initiative titled *Research on the Whole-Process Railway Noise Monitoring System and Implementation Path*. This initiative focuses on establishing a comprehensive, integrated system for monitoring railway noise throughout the entire operational process, from construction and testing phases to daily operations. The project not only seeks to advance noise monitoring technology but also aims to develop practical solutions for mitigating noise pollution in high-speed railway environments, ensuring both environmental sustainability and passenger comfort.

Railway Sciences
Vol. 3 No. 6, 2024
pp. 704-716
Emerald Publishing Limited
e-ISSN: 2755-0915
p-ISSN: 2755-0907
DOI 10.1108/RS-09-2024-0037

findings provide valuable insights for noise control and rail maintenance in the context of China's high-speed rail system.

Keywords High-speed railway, Rail, Acoustic roughness, Short-wavelength irregularity
Paper type Research paper

1. Introduction

The continuous and rapid development of China's high-speed railways has significantly contributed to the growth of the national economy and the improvement of people's lives. However, the associated vibration and noise problems have varying degrees of impact on both the external environment and the comfort within the train compartments (Thompson, 2000). With the construction of high-speed rail projects designed for speeds of 400 km/h and the gradual increase in operating speeds, the challenge of controlling wheel-rail vibration noise has become more critical.

International research on rail acoustic roughness spectra began with theoretical studies on wheel-rail rolling noise. Among these, the rolling noise models developed by Remington and Thompson, which are based on track irregularities in medium and low-speed lines, have been widely applied (Thompson, 1993; Remington, 1987a, b). However, these theoretical models were constructed for conventional ballasted tracks at speeds of 160 km/h or less (Stefanelli, Dual, & Cataldi Spinola, 2006). They were designed for specific wheel and track conditions and did not account for noise differences arising from the same wheelset operating on different rails (Sasakura & Sato, 2005). The train suspension parameters considered only the unsprung mass, and do not consider other crucial factors affecting wheel-rail interaction, such as sprung mass, primary suspension stiffness, and damping (Zhu, Liu, Wang *et al.*, 2020). The dynamics models and structural components involved were simplified, and the acoustic roughness spectrum data were measured under low-speed European conditions, making them inadequate for high-speed railways.

In recent years, China has gradually undertaken and deepened research on the acoustic excitation mechanisms of wheel-rail roughness. However, there is still a lack of systematic and comprehensive analysis and discussion regarding the roughness spectrum of high-speed railway rails (Zhang, Kang, & Liu, 2008). Moreover, the research on rail roughness in high-speed railways has been relatively short, and key parameters such as the combined wheel-rail roughness spectrum for high-speed railways have not yet been fully understood (Xiao, Yang, Zhang *et al.*, 2008). This has led to a lack of accurate input excitations for predicting wheel-rail rolling noise (Lian, Lu, Yang *et al.*, 2006). In summary, rail surface roughness is crucial for addressing the input sources of wheel-rail noise excitation. Research on the acoustic roughness spectrum of wheel-rail interactions, both domestically and internationally, includes three forms: separated spectra for wheels and rails, rail roughness spectra that do not consider wheel surface roughness (Chen, Zhang, & Lin, 2005), and combined wheel-rail roughness spectra (Liu & Wu, 2000). Although extensive testing and statistical analysis have been conducted on the roughness of wheels and rails both domestically and internationally, due to the relative scarcity of high-speed railway data abroad and the limited systematic research within China (Zeng, Wang, & He, 1996), there is no widely recognized acoustic evaluation method or control basis for rail roughness.

This paper systematically tests and analyzes rail roughness during the initial operation period and the service life of high-speed railways. Based on key aspects of the calculation and statistical methods for rail acoustic roughness spectra, the paper establishes a calculation methodology and workflow for high-speed rail acoustic roughness spectra. It also analyzes the probability distribution of the measured rail acoustic roughness spectra and, accordingly, determines an acoustic roughness excitation spectrum suitable for China's high-speed railways. This effectively describes the acoustic roughness characteristics of high-speed railways and provides crucial input for the accurate prediction of wheel-rail noise in high-speed railways.

2. Data sources

China's high-speed rail network is extensive, with varying construction methods, track structures, train types, speed levels, and environmental conditions, leading to significant variability in rail roughness data. To systematically understand the roughness characteristics of China's high-speed railway rails, this study considers factors such as line grade, years of operation, track structure, and operational environment. It analyzes the surface roughness characteristics of rails during the operational period on typical line segments. Long-term monitoring and testing were conducted on major high-speed railway lines in China, including the Beijing-Shanghai, Beijing-Guangzhou, Beijing-Harbin, and Dandong-Dalian lines, to identify the roughness characteristics of typical high-speed railway rails.

2.1 Testing methods

The general definition of rail surface roughness refers to the small spacing and minor peak-valley irregularities on the machined surface, reflecting the precision and smoothness of rail processing. However, from an acoustic research perspective, the acoustic roughness of wheels and rails is not solely concerned with the physical characteristics of the surface finish, but focuses more on the irregularities during the idealized contact and rolling process between the wheel and the rail, particularly in terms of their contribution as acoustic excitation sources. In this context, contact filtering effects are not considered, and the surface irregularity data obtained from testing are acoustically adjusted to more accurately reflect their impact on wheel-rail noise.

To obtain precise data on wheel-rail acoustic roughness, this study employed the BBM wheel-rail roughness testing system for on-site measurements on high-speed railway lines. This system captures the microscopic irregularities of the rail surface and converts them into acoustic data, providing fundamental data support for subsequent noise analysis. The rail roughness field testing is shown in Plate 1, and the testing process strictly followed standard operational procedures to ensure the accuracy and reliability of the data. Through these test results, further analysis can reveal the specific mechanisms by which rail roughness affects high-speed railway noise.

Source(s): Authors' own work

Plate 1.
Rail roughness test

2.2 Data preprocessing methods

The measured rail roughness data often contain outliers due to factors such as sensor and signal transmission errors, as well as external interference. Additionally, since the acoustic roughness of the wheel-rail is related to the geometric position of the contact between the wheel and the rail surface irregularities, preprocessing and acoustic adjustments are required to remove outliers and improve calculation accuracy.

2.2.1 Peak removal. The acoustic roughness of the rail is meant to characterize the wavelength amplitude fluctuation characteristics of short-wavelength irregularities on the rail. The wheel-rail roughness testing uses an inertial coordinate method for measurement. The roughness data obtained from testing must first undergo outlier removal. For instance, during the testing process, sharp pits or protrusions on the rail surface may be encountered, as shown in Figure 1, which are often caused by surface contaminants or interference noise in the electrical signal. Such abnormal interference should be removed from the normal roughness data. In the frequency domain, these abnormal signals are characterized by a broadband random roughness component and large discrete components, as shown in Figure 2. These abnormal signals can be filtered out based on their spatial frequency domain characteristics. The roughness data before and after peak removal are shown in Figure 3.

As shown in Figure 3, after the peak removal process, the roughness amplitude in the short wavelength range (less than 20 cm) is significantly reduced, while the impact on the roughness amplitude for medium and long wavelengths (greater than or equal to 20 cm) is not noticeable.

2.2.2 Curvature correction. The roughness data obtained from rail roughness testing can reflect the flatness of the rail surface itself. However, as the initial irregularity acting as the excitation source for wheel-rail rolling noise, it is necessary to consider the geometric contact state between the wheel and the rail. When the wheel moves along the rail, the wheel's curvature is finite, and the micro-irregularities on both the wheel and the rail surfaces cannot fully contact each other. Specifically, the troughs of irregularities cannot make effective contact, and the wheel tends to "jump" from one peak of the micro-irregularities to the next adjacent peak. Therefore, the effective contribution of rail roughness is related to the wheel's curvature. By considering wheel curvature, roughness data corrected from the perspective of wheel-rail contact geometry can more accurately reflect the contribution of roughness to wheel-rail rolling noise. The principle of curvature correction is shown in Figure 4. For every

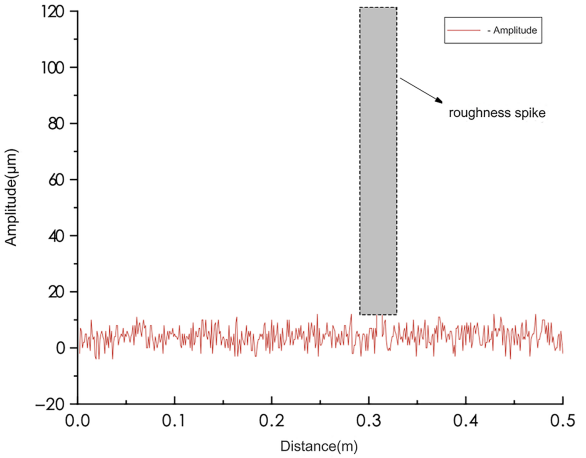

Source(s): Authors' own work

Figure 1.
Spatial domain characteristics of roughness peaks

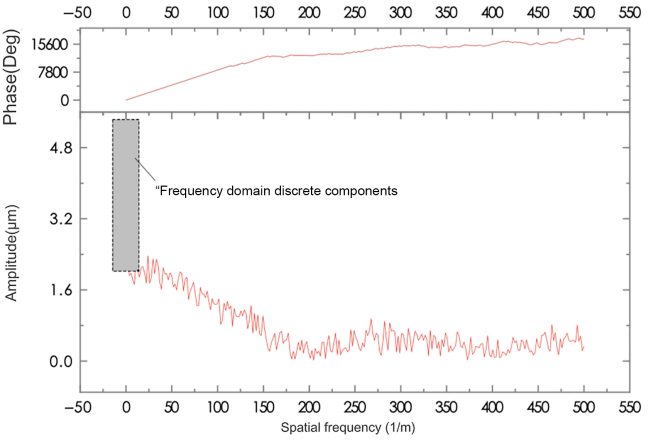

Source(s): Authors' own work

Figure 2.
Spatial frequency domain characteristics of roughness peaks

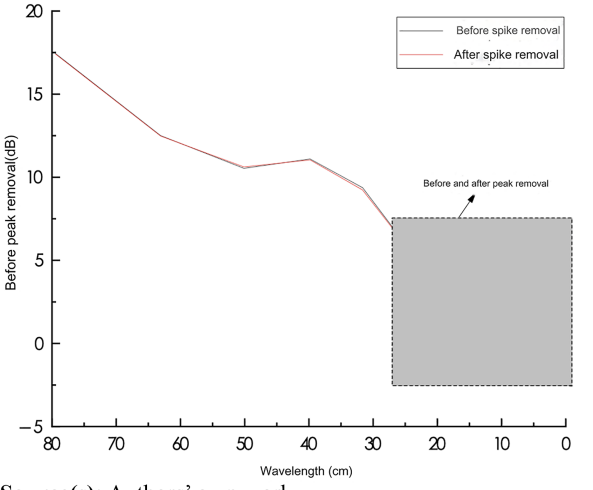

Source(s): Authors' own work

Figure 3.
Roughness data before and after peak removal

point coordinate x_i on the roughness surface $r(x)$, with the contact point located at the center x_0, and in relation to the ideal surface, the acoustic roughness is corrected by considering the measured wheel radius through curvature correction $r_k(x_i) = r'(x_i) - r(x_i)$.

The roughness data can be expressed as a function of the rail length. Its physical meaning is the variation of surface irregularities at different positions relative to the average trajectory, i.e. roughness amplitude. The logarithmic roughness level L_r^k is commonly used in research, defined as shown in Equation (1), with units in dB:

$$L_r^k = 10log\left(r_k^2 \Big/ r_{ref}^2\right) \tag{1}$$

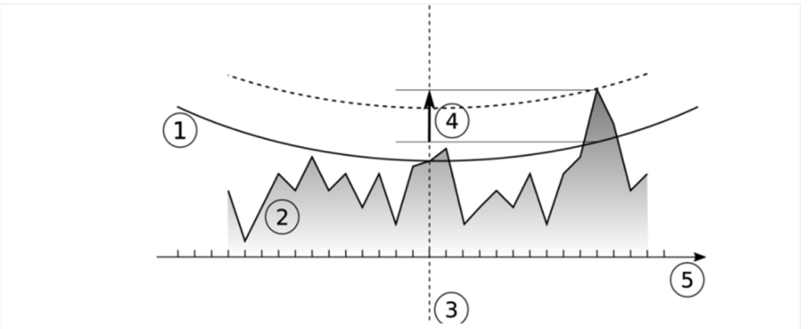

① Ideal wheel surface; ② Actual wheel roughness $r(x)$; ③ Contact center point x_0; ④ Acoustic roughness r_k; ⑤ Sampling point x_i

Source(s): European Committee for Standardization (2009)

Figure 4.
Geometric relationship between wheel and rail roughness

When making corrections, quantification is required in 1/3 octave bands r_{ref}, with a reference value of 1μm. The squares of the obtained narrowband spectrum amplitudes are summed in each one-third octave band and divided by the number of calculation points to obtain the octave band statistics. In the definition of acoustic roughness, the effective amplitude (root mean square value) of 10μm roughness corresponds to a roughness level of 20 dB, while the roughness amplitude of 1μm corresponds to a roughness level of 0 dB. The roughness data obtained after curvature correction is shown in Figure 5.

As shown in Figure 5, after applying curvature correction to the roughness data, there is a significant reduction in the roughness amplitude for medium and long wavelengths (greater than 20 cm). For short wavelengths (less than or equal to 20 cm), the amplitude increases in some wavelength segments, while the effect on roughness amplitude for very short wavelengths is not noticeable.

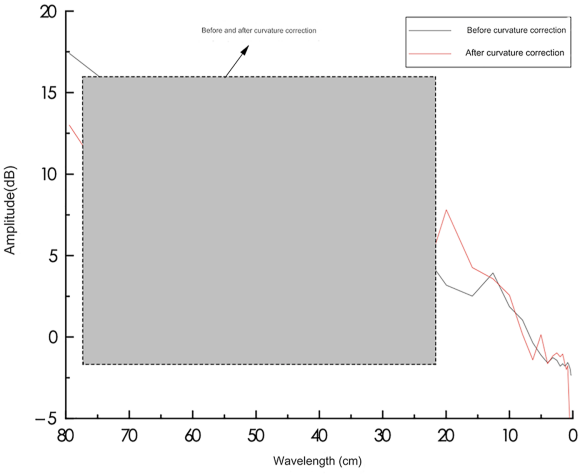

Source(s): Authors' own work

Figure 5.
Roughness data before and after curvature correction

2.2.3 Spatial-wavelength domain transformation. When calculating rail roughness, the long-distance test data needs to be segmented for processing. To avoid distortion in the wheel-rail roughness spectrum, it is necessary to apply windowing to the finite-length roughness data, and the choice of window function is critical to data processing. By comparing the effects of the Hanning window and the Tukey window on data processing, as shown in Table 1, the rail roughness of typical high-speed railways can generally be regarded as a stationary random signal. The Hanning window assigns greater weight to the data in the middle and less to the data at both ends, making it well-suited for processing such roughness characteristic signals.

3. Distribution pattern of rail acoustic roughness

To develop an acoustic roughness spectrum for high-speed railway rails, it is necessary to perform a statistical analysis on the measured rail roughness data after acoustic filtering. This analysis should focus on the primary and secondary rail lines in China's high-speed railway network to clearly determine the distribution patterns of rail roughness. Based on these patterns, a non-parametric test is conducted on the roughness data, ultimately yielding a reasonable and accurate acoustic roughness spectrum for high-speed railway rails.

Multiple measurements were taken on typical sections of several high-speed railway lines in China during their operational periods. The results underwent statistical analysis, and after acoustic processing, it was observed that the statistical distribution of acoustic rail roughness across different wavelengths generally followed a normal distribution. By calculating the frequency of roughness amplitudes for each wavelength, the overall relative frequency distribution was obtained, with the relative frequency of roughness amplitudes at certain wavelengths shown in Figure 6.

For each wavelength, the squared sum of the roughness amplitudes was calculated, and the distribution pattern was analyzed. The trend of the distribution is illustrated in Figures 7 and 8. Statistical data analysis revealed that the complete set of roughness data, obtained from several railway sections under various conditions, conforms to a χ^2 distribution with 6 degrees of freedom. This distribution model provides a reliable foundation for describing the acoustic roughness characteristics of high-speed railway rails.

4. Compilation and characterization of rail acoustic roughness spectrum

4.1 Calculation method and steps

The measured wheel-rail roughness acoustic spectrum data was statistically analyzed. Taking the rail roughness data processing method as an example, the specific process is as follows.

(1) The measured roughness data of several sections of high-speed railway lines are subjected to curvature correction and peak removal to obtain the time domain signal after acoustic filtering. The long sequence signal in the time domain is then subjected to short-time Fourier transform to obtain the wavelength-amplitude correspondence of the roughness in the wavelength domain.

Window function	Main Lobe width (°)	Leakage factor (%)	Side Lobe/Main Lobe peak ratio (dB)
Hanning	$8\pi/N$	0.05	−31.5
Tukey	$40\pi/9N$	6.98	−13.5

Source(s): Authors' own work

Table 1. Comparison of window functions

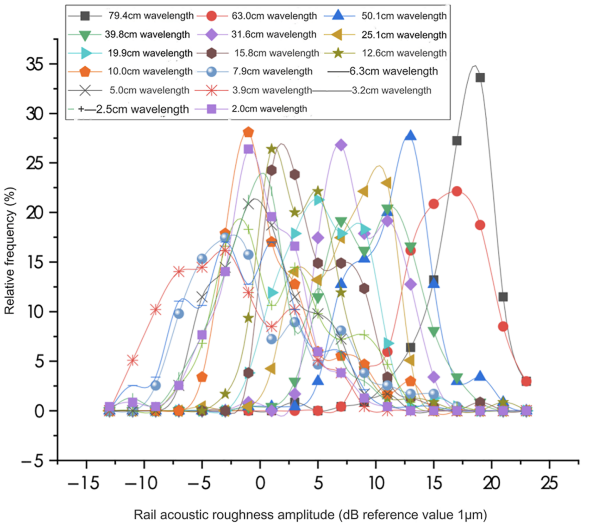

Source(s): Authors' own work

Figure 6.
Distribution pattern of roughness amplitude at various wavelengths—follows a general normal distribution

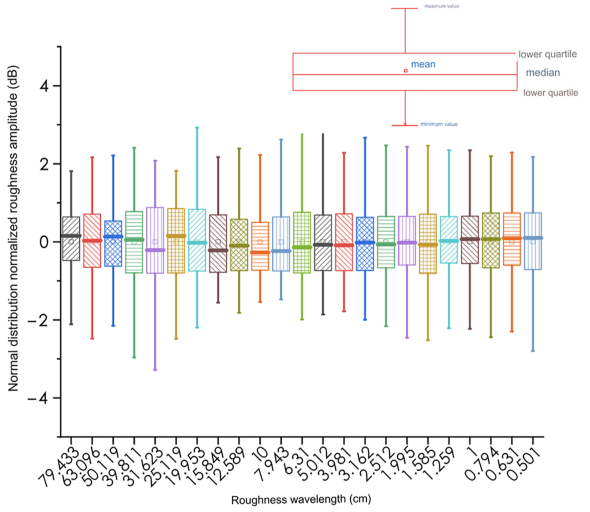

Source(s): Authors' own work

Figure 7.
Box plot of total rail roughness distribution

(2) Statistical analysis was performed on the wavelength domain roughness amplitude data, that is, the frequency and relative frequency calculations were performed on the roughness amplitude distribution trends at each wavelength. It was shown that the roughness amplitude at a single wavelength conforms to the general normal distribution law under large sample statistics of major high-speed rail lines.

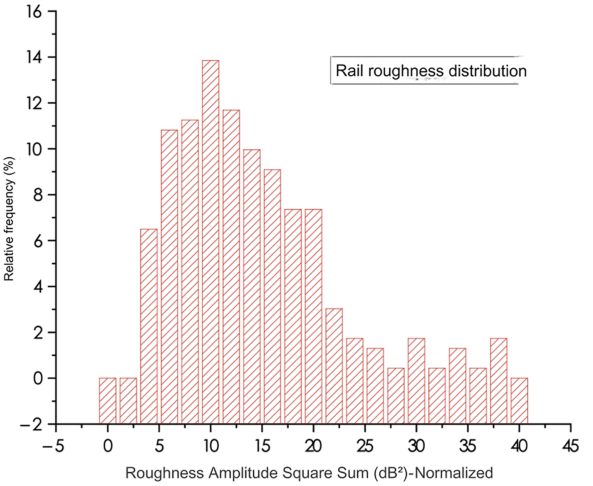

Figure 8.
Overall distribution pattern of rail roughness

Source(s): Authors' own work

(3) The general normal distribution function of the roughness amplitude under a single wavelength is normalized to obtain the data statistical results under the standard normal distribution N (0, 1). The roughness standard normal distribution N (0, 1) results under a single wavelength obtained by processing several sections of the line are recorded as a random variable ξ_i. Then, several roughness data under n wavelengths constitute n independent random variables $\xi_1, \xi_2, \ldots\ldots \xi_i \ldots$, and each random variable conforms to the standard normal distribution.

(4) According to χ^2 the definition of distribution, if n independent random variables $\xi_1, \xi_2, \ldots\ldots \xi_i \ldots$ conform to the standard normal distribution, then the sum of the squares of these n random variables that conform to the standard normal distribution constitutes a new random variable Q, as shown in Equation (2):

$$Q = \sum_{i=1}^{n} \xi_i^2 \tag{2}$$

Its distribution law conforms to χ^2 the distribution, recorded as $Q \sim \chi^2(v)$ or $Q \sim \chi_v^2$ (where v = n-k, k is the number of constraints). According to large sample statistics, it is believed that the entire set of roughness data obtained from actual measurements of several sections of line conditions conforms to the distribution law with 6 degrees of freedom χ^2.

(5) The Kolmogorov-Smirnov non-parametric test was performed on the entire set of roughness data obtained from the tests on each section to eliminate abnormal section data in the roughness test.

(6) According to χ^2 the distribution law, the roughness test data at the significance level of 0.05 (confidence level of 95%) are statistically taken as typical values to form a valid set of roughness tests.

(7) The mean, median and standard deviation of the roughness amplitude at each wavelength in the effective set are calculated, and finally the measured acoustic roughness spectrum of my country's high-speed railway is formed.

4.2 Rail acoustic roughness spectrum

According to the calculation method described in Section 4.1, χ^2 the Kolmogorov-Smirnov non-parametric test was performed according to the distribution law with 6 degrees of freedom. After eliminating abnormal data, the rail acoustic roughness data at the significance level of 0.05 (confidence level of 95%) were statistically analyzed to obtain the effective set of rail acoustic roughness data in China, among which some rail roughness data are shown in Figure 9.

The acoustic roughness data of the rails in the effective set were further calculated and analyzed, and the mean, median and standard deviation of the roughness amplitude at each wavelength were calculated, as shown in Table 2.

Based on the statistical results of China's high-speed railway acoustic roughness in Table 2, the acoustic roughness spectrum of China's high-speed railway is plotted, as shown in Figure 10.

As shown in Figure 10, the acoustic roughness spectrum of China's high-speed railway rails obtained through statistical analysis shows that the mean and median are relatively close, with the two being almost identical for wavelengths greater than 15.8 cm. For wavelengths between 12.6 cm and 6.3 cm, the mean is slightly greater than the median. For wavelengths less than 6.3 cm, the two are relatively close. Because the acoustic roughness spectrum of the rails is used primarily for predicting wheel-rail noise in high-speed railways, the slightly higher mean spectrum is taken as the final acoustic roughness spectrum of China's high-speed railway rails, with the wavelength axis rounded, as shown in Figure 11.

As shown in Figure 11, the compiled acoustic roughness spectrum of China's high-speed railway rails covers wavelengths from 0.5 cm to 79 cm, corresponding to noise excitation frequencies of 123 Hz to 19.444 kHz at a speed of 350 km/h. The acoustic roughness spectrum primarily describes short and ultra-short wavelength roughness within 80 cm, where long

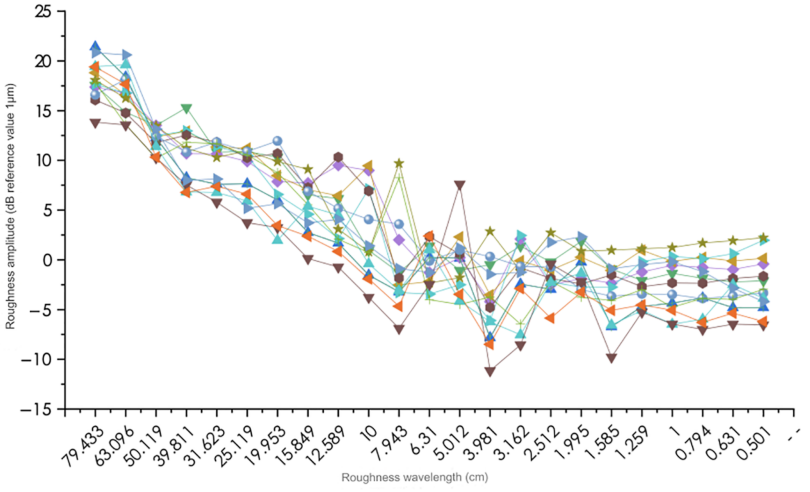

Source(s): Authors' own work

Figure 9.
Acoustic roughness data after statistical analysis

Wavelength (cm)	Mean (dB)	Standard deviation (dB)	Median (dB)
79.433	18.7	1.9	18.5
63.096	16.9	2.6	16.8
50.119	11.7	2	12
39.811	9.9	2.5	9.6
31.623	9.1	2	8.7
25.119	8.3	2.6	8.7
19.953	6.7	2.5	6.3
15.849	4.8	2.5	4.9
12.589	4	3.2	2.9
10	1.3	3.6	0.8
7.943	−0.6	4.6	−2.3
6.31	2.1	5.2	0.5
5.012	0.5	4.4	0.2
3.981	−4.1	4.1	−4.5
3.162	−2.4	3.1	−2.4
2.512	0.1	3.9	−0.6
1.995	0	3	−0.1
1.585	−3.4	3	−2.8
1.259	−1.3	2.6	−1.1
1	−2	3.3	−2.8
0.794	−2.6	2.7	−2.2
0.631	−2.1	2.5	−2.1
0.501	−2.6	3	−2.8

Source(s): Authors' own work

Table 2.
Statistical results of acoustic roughness for high-speed railway rails

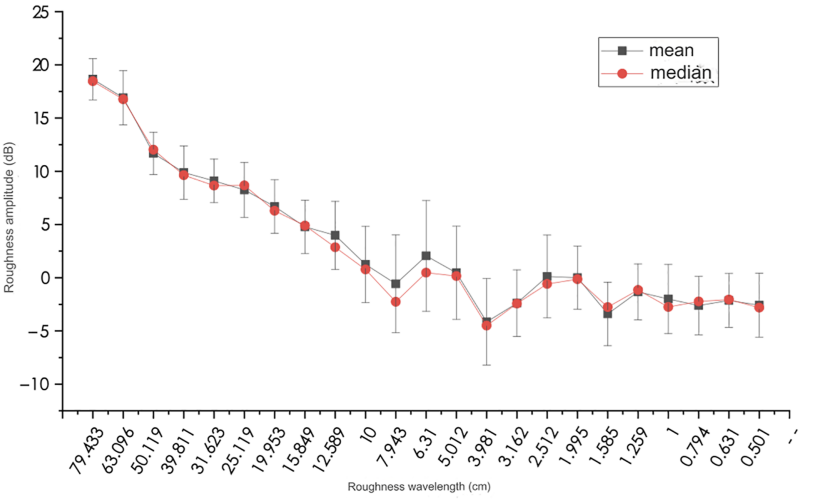

Source(s): Authors' own work

Figure 10.
Acoustic roughness spectrum of high-speed railway rails (mean + median)

wavelength roughness is more related to track irregularity quality, and low-frequency noise in high-speed railways is mainly dominated by aerodynamic noise. The 123 Hz corresponding to the 79 cm wavelength can meet the analysis requirements for low-frequency noise from wheel-rail interactions; the upper limit of high-frequency noise at

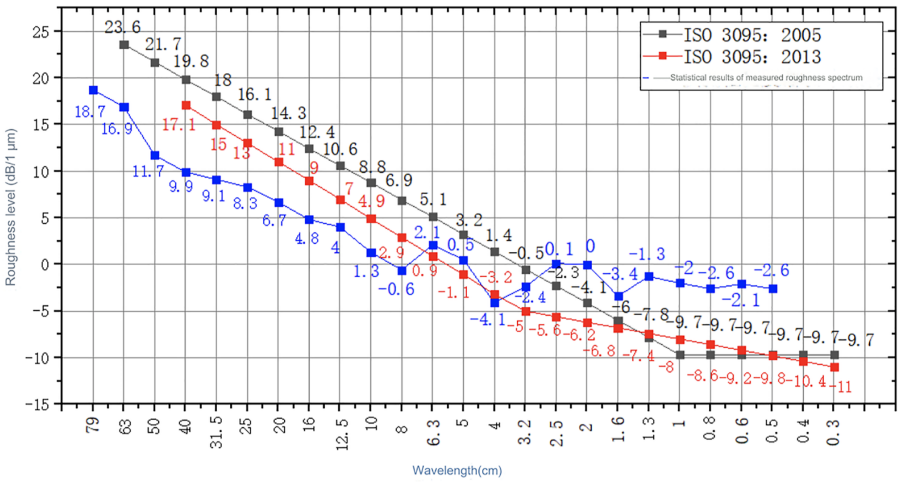

Source(s): Authors' own work

Figure 11.
Statistical results of measured acoustic roughness spectrum of rails

0.5 cm wavelength corresponding to 19.444 kHz can also meet the analysis requirements for high-frequency noise from wheel-rail interactions. The main reasons are as follows: first, according to the analysis of the measured exterior noise of China's high-speed railway, the noise attenuates rapidly above 5,000 Hz, and high-frequency noise above 10,000 Hz contributes little to high-speed rail noise; second, the upper limit of human hearing is 20,000 Hz, which is close to 19.444 kHz. Therefore, it is more appropriate to set the wavelength of the acoustic roughness spectrum of my country's high-speed railway rails to 0.5cm~79cm.

At the same time, compared with the provisions on rail roughness limits in ISO 3095:2005 and ISO 3095:2013 standards issued by the International Organization for Standardization in Figure 11, China's rail acoustic roughness spectrum is smaller than the ISO limit in the wavelength range greater than 8 cm, is equivalent to or between the ISO 3095:2005 and ISO 3095:2013 limits in the wavelength range of 3.2 cm to 6.3 cm, and is larger than the ISO limit in the wavelength range less than 2.5 cm.

5. Summary

Based on extensive and long-term tracking measurements of rail roughness on China's high-speed railway, this paper reveals the statistical patterns of rail roughness within short and very short wavelength ranges. It also studies the data processing and statistical methods for constructing the acoustic roughness spectrum of rails and has developed an acoustic roughness spectrum specifically suited to China's high-speed railway system. This spectrum provides reliable measured excitation source input for high-frequency vibration and noise simulation in the design of Chinese high-speed trains and offers strong technical support for noise and vibration control in high-speed railways. Additionally, the findings of this study lay a solid foundation for the future development of high-speed rail technology, particularly in innovative applications related to noise and vibration control, thus promoting further advancements and optimization in China's high-speed rail sector.

References

Chen, C., Zhang, J., & Lin, J. (2005). Robust parameter estimation and spectral analysis of track irregularity signals. *China Railway Science*, 03, 73–76.

Lian, S., Lu, H., Yang, W., & Zong. (2006). Track irregularity analysis program. *China Railway Science*, (01), 68–71.

Liu, X., & Wu, W. (2000). Power spectrum analysis of short-wave irregularity of rail welding joints. *China Railway Science*, 02, 28–36.

Remington, P. J. (1987a). Wheel/rail rolling noise I: Theoretical analysis. *Journal of the Acoustical Society of America*, *81*(6), 1805–1823. doi: 10.1121/1.394746.

Remington, P. J. (1987b). Wheel/rail rolling noise II: Validation of the theory. *Journal of the Acoustical Society of America*, *81*(6), 1824–1832. doi: 10.1121/1.394747.

Sasakura, M., & Sato, K. (2005). Acoustic characteristics of railway wheels with different web shapes. In *The Proceedings of the Dynamics & Design Conference* (pp. 356–1).

Stefanelli, R., Dual, J., & Cataldi Spinola, E. (2006). Acoustic modeling of railway wheels and acoustic measurements to determine involved eigenmodes in the curve squealing phenomenon. *Vehicle System Dynamics*, *44*(sup1), 286–295.

Thompson, D. J. (1993). Wheel/rail noise generation, part II: Wheel vibration. *Journal of Sound and Vibration*, *161*(3), 421–446. doi: 10.1006/jsvi.1993.1083.

Thompson, D. J., & Jones, C. (2000). A review of the modeling of wheel/rail noise generation. *Journal of Sound and Vibration*, *231*(3), 519–536. doi: 10.1006/jsvi.1999.2542.

Xiao, S., Yang, G., Zhang, W., & Zhao, Y. (2008). Simulation of random track irregularities based on spectral density function. *China Railway Science*, (02), 28–32.

Zeng, Y., Wang, W., & He, Q. (1996). Time-frequency conversion reproduction technology of vehicle excitation spectrum. *China Railway Science*, 04, 26–32.

Zhang, S., Kang, X., & Liu, X. (2008). Analysis of track irregularity spectrum characteristics of Beijing-Tianjin intercity railway. *China Railway Science*, 05, 25–30.

Zhu, Z., Liu, Y., Wang, L., Wang, F., & Wang, D. (2020). Random vibration analysis of subway transportation sites based on 2.5D finite element method and virtual excitation method. *China Railway Science*, *41*(04), 29–39.

Further reading

European Committee for Standardization (2009). *EN 15610:2009 - railway applications - noise emission - rail roughness measurement related to rolling noise generation*. CEN.

Poisson, F., Gautier, P. E., & Letourneaux, F. (2007). Noise sources for high-speed trains: A review of results in the TGV case. In *Proceedings of the 9th International Workshop on Railway Noise* (pp. 71–77) Munich: Springer.

Remington, P. J. (1976a). Wheel/rail noise, part I: Characterization of the wheel/rail dynamic system. *Journal of Sound and Vibration*, *46*(3), 359–379. doi: 10.1016/0022-460x(76)90861-0.

Remington, P. J. (1976b). Wheel/rail noise, part IV: Rolling noise. *Journal of Sound and Vibration*, *46*(3), 419–436. doi: 10.1016/0022-460x(76)90864-6.

Corresponding author

Chenge Wang can be contacted at: paigewang@qq.com